Journal of Thermal Analysis and Calorimetry, Vol. 59 (2000) 245–255

Dedicated to Prof. Edith A. Turi in recognition of her leadership in education

STRUCTURAL DEVELOPMENT DURING THERMAL FRACTIONATION OF POLYETHYLENES

W. Liu[1], *S. Kim*[1], *J. Lopez*[1], *B. Hsiao*[1*], *M. Y. Keating*[2], *I.-H. Lee*[2], *B. Landes*[3] *and R. S. Stein*[4]

[1]Chemistry Department, State University of New York at Stony Brook, Stony Brook NY 11794-3400
[2]E. I. duPont de Nemours and Company, Wilmington, DE 19880-0323
[3]Dow Chemical Company, Midland, MI 48667
[4]Chemistry Department, University of Massachusetts, Amherst, MA 01003, USA

Abstract

In this study, the stepwise isothermal crystallization or thermal fractionation of Ziegler–Natta and metallocene based polyethylenes (ZN-PE and m-PE) with two kinds of branch lengths (ethyl and hexyl) and branch compositions were studied using simultaneous synchrotron small-angle X-ray scattering (SAXS)/wide-angle X-ray diffraction (WAXD) and differential scanning calorimetry (DSC). The crystal long period and the invariant were determined by SAXS, and the variations of crystal unit cell parameters and the degree of crystallinity were determined by WAXD. The arithmetic mean length (*Ln*), the weighted mean length (*Lw*) and the broadness index (*Lw*/*Ln*) of the studied polyethylenes were previously determined by DSC. Results from these studies were interpreted using the model of branch exclusion, which affects the ability of the chain-reentry into the crystal phase. Multiple SAXS peaks and step-change in crystallinity change (WAXD) were seen during heating, which corresponded well with the crystal thickness distribution induced by stepwise crystallization. The effects of the heterogeneity of the 1-olefin branch length and the distribution on the crystal long period and the invariant as well as the degree of crystallinity were discussed.

Keywords: DSC, metallocene, polyethylenes, SAXS, synchrotron radiation, thermal fractionation, WAXD, Ziegler–Natta

Introduction

The studies of the effects of chain branching on the crystallization behavior in metallocene ethylene 1-olefin copolymers (m-PEs) as compared to the conventional Ziegler–Natta polyethylenes (ZN-PEs) have grown significantly since the introduction of metallocene catalytic copolymerization in industrial applications [1–3]. The studies of the chain branch distribution and the sequence length between the chain branches have been carried out with temperature rising elution fractionation (TREF), differential scan-

* Author for correspondence: e-mail: bhsiao@notes.cc.sunysb.edu

1418–2874/2000/ $ 5.00
Akadémiai Kiadó, Budapest

ning calorimetry (DSC), temperature modulated DSC (MDSC), carbon-13 NMR and solvated thermal analysis fractionation (STAF) [4–12]. The stepwise isothermal segregation technique (SIST) has turned out to be a useful method to differ molecular weight and molecular weight distribution, and distribution of side branches, all of which can affect the crystalline structure or size of crystallites. For example, Keating *et al.* [13, 14] evaluated the comonomer distribution in ethylene copolymers using a DSC stepwise isothermal fractionation method and estimated the crystalline ethylene sequence lengths. Starck *et al.* [15] used both SIST and TREF to study the comonomer distributions of commercial linear low-density polyethylene (LLDPE) and linear very low- density polyethylene (VLDPE) produced with traditional high activity Ziegler–Natta catalysts. They concluded that SIST is a tool for the qualitative analysis of the chemical composition distribution and is useful to characterize the heterogeneity in the comonomer unit distribution. Wolf *et al.* [16] identified and distinguished between different types of low-density polyethylene (LDPE) based on the thermal fractionation technique with FTIR measurements.

Thermal fractionation is a temperature-dependent segregation process based on recrystallization and reorganization of the crystallizable segments of the polyethylene backbone in the melt. Compared to TREF, its segregation mode is different in that there is no actual physical separation of the macromolecules. The technique uses the hypothesis that only ethylene sequences above a certain critical length between the branches can participate in the crystallization process. In this case, the short branches (≥ethyl branch length) are large enough to be excluded from the crystalline phase of the ethylene sequence.

In this study, we employ stepwise isothermal fractionation together with synchrotron simultaneous small-angle X-ray scattering (SAXS) and wide-angle X-ray diffraction (WAXD) to study both m-PE and ZN-PE with different comonomer type and content. Our objective is to understand how the thermal fractionation can affect crystallinity unit cell parameters, and morphological variables, as this information is not available in the literature today. The lack of such information has often cast some doubts in the use of thermal fractionation to determine the molecular parameters.

Experimental

Four polyethylene samples were commercially obtained from the various polyethylene suppliers. Table 1 lists the information on the catalyst types, melt indices, densities, comonomer types and comonomer contents of these PEs. The comonomer contents reported in Table 1 were quantitatively determined by ^{13}C NMR at 100 MHz and 140°C with a concentration of 10% polymer in a 6/1 trichlorobenzene/benzene-d_6 solvent system containing $Cr(AcAc)_3$ as a relaxation agent. The crystallinity of the films, extruded at melt temperature between 280 and 300°C with the speed of 5–9 feet per minute, was determined by the enthalpy of fusion in DSC based on ΔH=290 J g^{-1} for 100% crystalline polyethylene, which is shown in Table 2.

Table 1 Ethylene based polymers in this study

PE sample	Catalyst type	Comonomer type	MI/190°C	Density/ g ml^{-1}	1-olefin/ mol%
Sclair 11E1	Z. N.	C4[a]	1.4	0.920	3.3
Attane 4201	Z. N.	C8[b]	1.0	0.912	4.2
Exact 3027	met	C4	3.5	0.900	6.0
Affinity 1140	met	C8	1.6	0.899	6.2

[a]the branch length is C2 (ethyl); [b]the branch length is C6 (hexyl)

In this study, the PE samples were first heated to 175°C and held for 5 minutes, then cooled rapidly to 130°C and held for 12 hours. The stepwise crystallization process was repeated by annealing in a 10°C decrement until 30°C. The time for each stage where the samples were held for stepwise crystallization varied: 12 h for 130, 120, 110 and 100°C; 8 h for 90, 80, 70, 60°C; 6 h for 50, 40 and 30°C. The DSC profiles of the thermally fractionated PE samples were first recorded individually using a Perkin Elmer DSC7 station calibrated with indium and mercury under a nitrogen environment at 2.5°C min^{-1} rate from 25 to 175°C.

Table 2 Physical parameters of polyethylene samples

PE sample	*Ln* ethylene repeat	*Lw* ethylene repeat	*Lw/Ln*	X_c^a/%	X_c^b/%
Sclair 11E1	44.35	58.84	1.33	45.1	43.1
Attane 4201	39.70	60.19	1.52	37.4	31.5
Exact 3027	18.97	21.87	1.15	30.1	14.2
Affinity 1140	19.03	20.73	1.09	27.6	15.7

[a]Crystallinity of the as-extruded film determined from enthalpy of fusion between 20°C and the last crystal disappearing temperature in DSC; [b]Crystallinity of thermally fractionated PEs obtained by dividing the sum of the crystalline diffraction peak areas to overall diffraction area in the WAXD analysis

The melting study of PEs using simultaneous synchrotron SAXS and WAXD techniques was carried out at the Advanced Polymers Beamline (X27C), in National Synchrotron Light Source (NSLS), Brookhaven National Laboratory (BNL). Two position sensitive detectors (European Molecular Biology Laboratory, EMBL) were used to detect the SAXS and WAXD profiles simultaneously. The chosen wavelength was 0.1307 nm, the sample to detector distance for SAXS was 1590 mm and for WAXD was 184.7 mm, and the data acquisition time was 20 seconds per scan. The specimen was heated from 25 to 175°C also with a heating rate of 2.5°C min^{-1}. All measured intensities were corrected for beam fluctuation and sample absorption.

Results and discussion

As indicated earlier, multiple endotherms of thermally fractionated samples may provide information on the ethylene sequence length and distribution between the branch points. In Fig. 1, two typical DSC heating scans of thermally fractionated PE samples (ZN-PE, Attane 4201 and m-PE, Exact 3027) are shown, which illustrates how the different catalyst type can vary significantly between two kinds of polymers. It is known that the multiple active sites in the conventional Ziegler–Natta catalysts polymerize by inserting the 1-olefin comonomer at relatively irregular intervals to the growing ethylene chains, resulting in a broad and heterogeneous branching distribution of short branches in polyethylene. The single site metallocene catalysts, by contrast, are able to incorporate the 1-olefin comonomer into the ethylene chains rather homogeneously and produce a relatively narrow molecular weight distribution. As a result, the nominal melting temperature of ZN-PE is significantly higher than that of m-PE, which is in agreement with Fig. 1. The change of the different type of branches (ethyl and hexyl) does not seem to affect the step crystallization and subsequent melting behavior in the chosen four polymers. In Fig. 1, it is seen that the thermal fractionation technique induces multiple endotherms in DSC curves. In spite of a more homogeneous structure in m-PE, this single site copolymer also shows multiple endotherms at lower temperatures, which indicates a shorter and narrow distribution of ethylene sequences between the branches. The principle of the thermal fractionation method has been explained earlier. As the molten polymer is held at the highest crystallization temperature, the longest crystallizable sequences can crystallize first. The 12 h crystallization time should allow the crystallization to complete. With each successively decreasing crystallization temperature, shorter sequence chains can progressively crystallize out at each stage. As a result, an in-situ fractionated sample, segregated by the sequence length, is obtained. The solidified longer segments probably lay

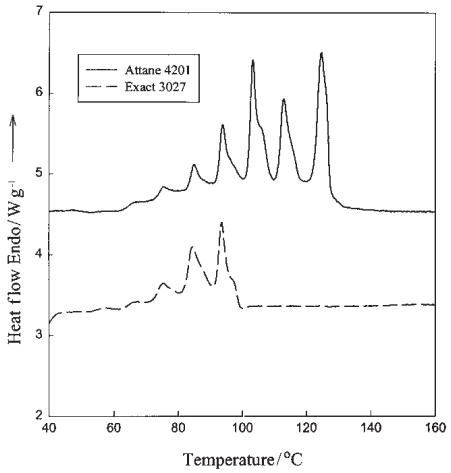

Fig. 1 DSC curves obtained from thermally fractionated PEs with melting rate of 2.5°C min^{-1}

out the crystalline network; thus it is not always possible for the shorter segments to be grouped by the exact lengths. The fractions of the segregated polymer thus are indicative by the multiple endotherms of the DSC scan [13, 14, 17].

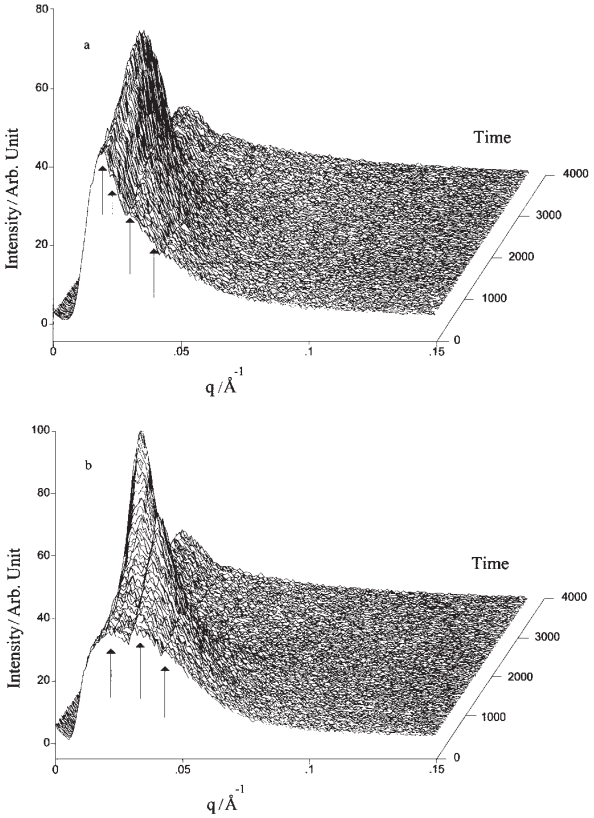

Fig. 2 SAXS profiles of thermally fractionated PEs, a) Ziegler–Natta based PE, Attane 4201; b) metallocene based PE, Exact 3027 heated from 25 to 175°C at rate of 2.5°C min^{-1}

The sequence lengths may be estimated from the melting points of the fractions, which have been demonstrated by Keating *et al.* [13] with the calibration of known hydrocarbons and HDPE. The definition of the arithmetic mean length (*Ln*), the weighted mean length (*Lw*) and the broadness indices (*Lw*/*Ln*) based on moments has been given in a previous paper [13]. Since the branch points interrupting the crystalline ethylene runs are defined by 1-olefin comonomers, these terms provide a statistical measure of the sequence distribution in the polymer. The statistical lengths and distribution, *Ln*, *Lw*, *Lw*/*Ln*, of the chosen samples are given in Table 2. The mean crystallizable ethylene lengths, as described by *Ln*, shorten with the increasing comonomer content as expected. The Ziegler–Natta 1-butene (ZN-C4) and 1-octene

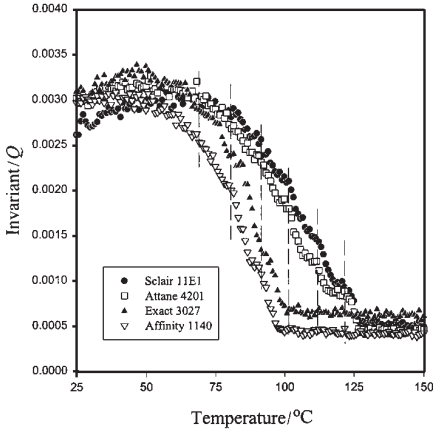

Fig. 3 Invariant *Q vs*. temperature of thermally fractionated PEs from the SAXS profiles in Fig. 2

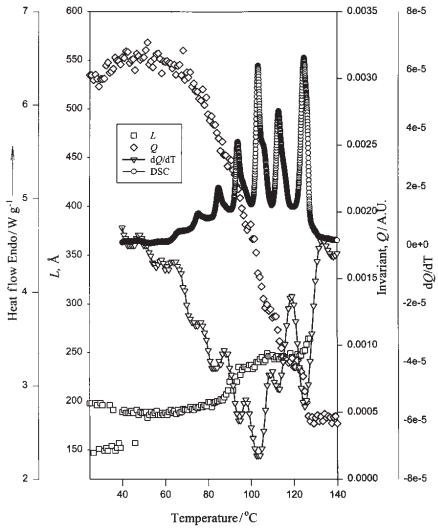

Fig. 4 Long period *L* and the derivative of the invariant d*Q*/d*T* during heating of thermally fractionated ZN-PE, Attane 4201, at a rate of 2.5°C min^{-1}. DSC curve and invariant *Q* of Attane 4201 were used for comparing with d*Q*/d*T* and the change of *L*

(ZN-C8) polyethylenes have the longer average length at 44 and 39 ethylene repeats and the very broad indices at 1.33 and 1.52. These long sequences contribute to the high crystallinity and resin stiffness. The metallocene 1-butene (m-C4) and 1-octene (m-C8) polyethylenes in this study have much shorter ethylene sequences with almost the same ethylene repeats, 19, and narrow sequence length distribution indices of 1.15 and 1.09. This is to be expected; the thermal fractionation process excludes

the side groups, the ethyl and hexyl branches (1-butene and 1-octene PE samples), from the crystal structure. At the equivalent molar content, the copolymers should have the same mean crystallizable sequence lengths and broadness indices regardless of the side chain length.

Figure 2 shows the typical SAXS profiles of two fractionated PE samples during heating at a rate of 2.5°C min^{-1}. Multiple peaks in the SAXS profiles indicated by the arrows are seen in both fractionated Ziegler–Natta (Fig. 2a) and fractionated metallocene (Fig. 2b) PE samples. The multiple SAXS peaks indicate that different lamellar thicknesses and long periods exist in the fractionated PE samples. The effects of the thermal fractionation on the distribution of the long period can also be found by comparing ZN-PE with m-PE. The broad first scattering peak and the stronger second scattering peak of the fractionated m-PE indicates that the thermal fractionation cannot produce many uniform thickness distributions in m-PE as in ZN-PE. This is consistent with the narrow sequence length distribution of m-PE. The corresponding plot

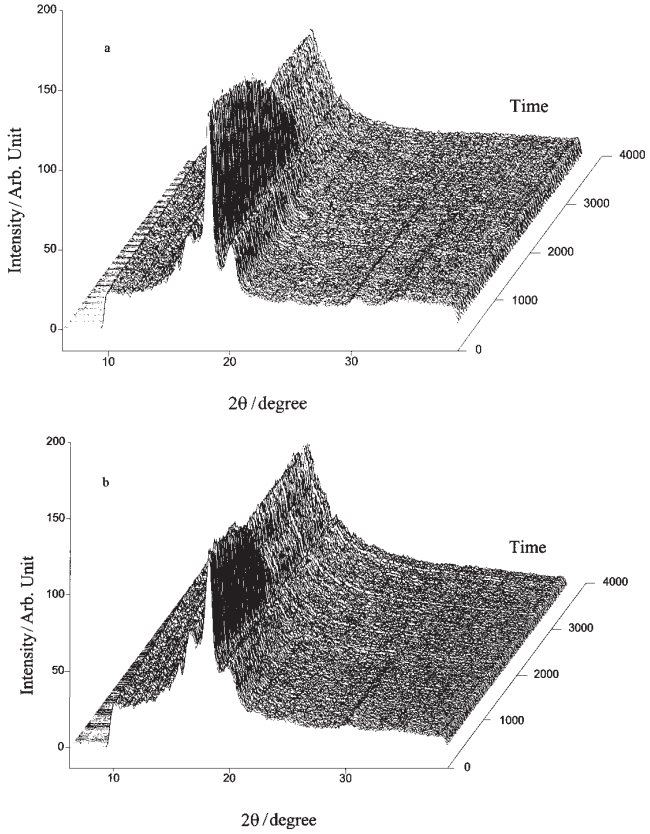

Fig. 5 WAXD profiles of thermally fractionated PEs, a) Ziegler–Natta based PE, Attane 4201; b) metallocene based PE, Exact 3027, heated from 25 to 175°C at a rate of 2.5°C min^{-1}

of the invariant during heating of the fractionated samples is shown in Fig. 3. It is seen that there are many step decreases in the change of the invariant as a function of temperature, which correspond well with the peaks in the DSC curve indicated by the vertical dash lines. This is seen more clearly at the curve representing the first derivative of the invariant Q with respect to temperature, dQ/dT, which is also proportional to the heat exchange (Fig. 4). We will discuss this observation in detail later.

Figure 5 illustrates typical WAXD profiles in the melting process of thermally fractionated PE. With the increase in heating temperature, the intense [110] and [200] reflection peaks from the orthorhombic crystal structure begin to diminish. The corresponding amorphous peak is found to increase and broaden. The degrees of crystallinity for four samples are shown in Fig. 6. One interesting feature is that multiple step decreases (indicated by the vertical dash lines) can be found in Fig. 6. In agreement with the multiple melting peaks obtained by DSC, the degree of crystallinity, measured by WAXD, also decreases in a stepwise fashion. Values for the original crystallinity, and crystallinity after fractionation are shown in Table 2. The m-PEs have generally lower crystallinity than ZN-PEs, because of their shorter average ethylene sequence. The segmental length distribution in the metallocene PE samples is more uniform between the branch points, yet large fractions exist which are below the critical sequence length to crystallize at ambient temperature. By comparing the crystallinity change in Table 2, it is seen that both ZN-PE samples begin with higher order of crystallinity compared to the m-PE samples after thermal fractionation. The crystallinity values obtained from DSC and WAXD are in good agreement for ZN-PE, but the crystallinity from DSC appears to be significantly larger than that from WAXD for m-PE. This suggests that significantly recrystallization occurs during the heating of m-PE, but not ZN-PE.

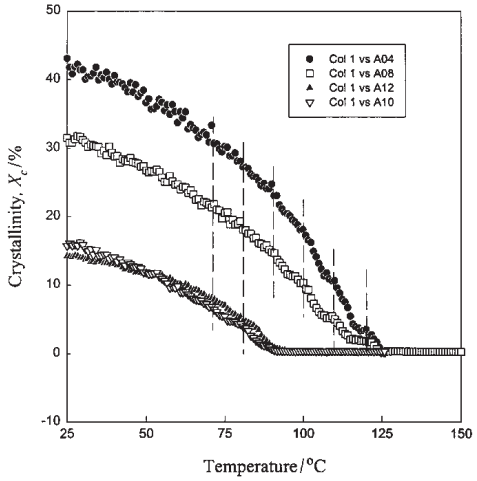

Fig. 6 The degree of crystallinity *vs*. heating temperature of thermally fractionated PEs from Fig. 5

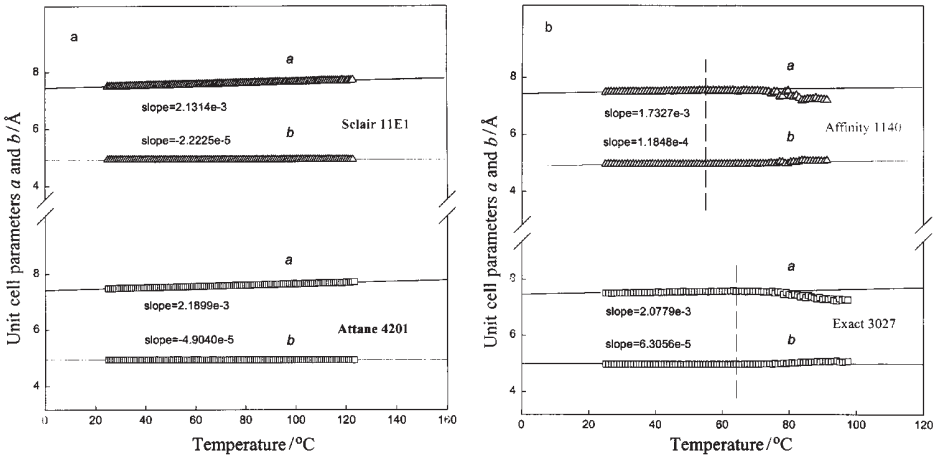

Fig. 7 Unit cell parameters (*a* and *b*) *vs*. heating temperature of (a) Ziegler–Natta based PEs and (b) metallocene based PEs

Evolution of the unit cell parameters of thermally fractionated PE samples during heating at a rate of 2.5°C min^{-1} is shown in Fig. 7. The unit cell parameter *a* of ZN-PE increases linearly with increasing melting temperature, but the unit cell parameter *b* decreases linearly. In contrast, upon heating of thermally fractionated m-PE samples, the unit cell parameters (*a* and *b*) first shows linear increase at lower melting temperature (from 25–55°C) with thermal expansion of *a* being larger than *b*. With the increase in temperature (>55°C), the unit cell *b* increases with temperature, while the unit cell parameter *a* of m-PE decreases significantly. This decrease in the unit cell parameter at higher temperatures indicates the process of crystal perfection or recrystallization of a more perfect structure. The difference in the changes of the unit cell parameters between ZN-PE and m-PE further indicates that thermal fractionation of ZN-PE produces more perfect crystal structure than that of m-PE, as significant crystal perfection occurs in the m-PE but not ZN-PE. The thermal coefficients of the unit cell parameters for the different samples are shown in Table 3. The magnitudes of these coefficients are consistent with those of linear polyethylene [18].

Table 3 Thermal coefficients for unit cell parameters of different polyethylene samples

PE sample	d*a*/d*T*/Å °C^{-1}	d*b*/d*T*/Å °C^{-1}
Sclair 11E1[a]	2.13e–3	–2.22e–5
Attane 4201[a]	2.19e–3	–4.90e–5
Exact 3027[b]	1.73e–3	1.18e–4
Affinity 1140[c]	2.08e–3	6.31e–5

[a]temperature range: 25–125°C; [b]temperature range: 25–55°C; [c]temperature range: 25–65°C

The DSC curve, the primary long period (L), the invariant (Q) and its first derivative during heating of a thermally fractionated ZN-PE, Attane 4201, at a rate of 2.5°C min^{-1} are shown in Fig. 4. It is very interesting to see that the first derivative of the invariant Q has the same number of peak, which is in total agreement with DSC endotherms. The invariant shows a comparatively small increase during heating from 25 to 80°C. According to the degree of crystallinity of Attane 4201 (Fig. 6) and the invariant relationship,

$$Q=KVX_{cL}(1-X_{cL})(\rho_c-\rho_a)^2$$

where K is a constant, V is the volume of the lamellar stacks, X_{cL} is the degree of crystallinity within the lamellar stacks, and ρ_c, ρ_a are the densities of the crystalline regions and the amorphous regions respectively, we conclude that the thinner crystal stacks formed with shorter sequence lengths melt first, which leads to the increase in the density difference between the crystalline and the amorphous regions (≤50°C). From 80 to 110°C, the large step increases in L and the significant step decreases in Q indicate that the melting takes place in the core structure of the lamellar stacks. Above 110°C, a continue decrease in Q and a smaller increase in L indicate that the remaining thicker lamellar stacks begin to melt, which causes the decrease in V. With the observation of X_c and the changes in unit cell parameters of a and b, we conclude that little crystal perfection takes place in the thermal fractionated ZN-PE sample while a considerable fraction of crystal perfection can occur in m-PE. These findings are consistent with the hypothesis of the DSC thermal fractionation stated earlier. Simultaneous measurements of SAXS and WAXD thus verify that the DSC thermal fractionation technique can resolve the sequence distribution in PEs.

Conclusions

Thermal fractionations of Ziegler–Natta and metallocene based polyethylenes with different branching lengths and compositions were measured using synchrotron X-ray (SAXS/WAXD) and DSC techniques. The properties of the crystalline and amorphous phases of metallocene and Ziegler–Natta polyethylenes are related to their structural differences. The crystallizable ethylene segments of ZN-C4 and -C8 polyethylenes have broader distribution and the average ethylene segments Ln are at least 2 times longer than their m-C4 and m-C8 counterparts in this study. We believe that ethyl and hexyl side groups are expelled to the surface of the crystals. Multiple-step decreases of the invariant Q measured by SAXS and the step-decrease in the degree of crystallinity obtained by WAXD indicated that thermal fractionation is an effective means to resolve the sequence distribution in both ZN-PE and m-PE. However, the thermal fractionation method is more effective in ZN-PE when the sequence distribution of the ethylene chains is broader and less effective in m-PE when the distribution is narrow.

We thank W. H. Shaw, Jr. for his contribution in analyzing the comonomer contents and types of polyethylene by ^{13}C-NMR. This work was supported in part by a grant from NSF (DMR 9732653), and in part by a DuPont Young Faculty Grant and a grant from DOW Chemical.

References

1 H. Sinn and W. Kaminsky, Adv. Organomet. Chem., 18 (1980) 99.
2 F. R. W. P. Wild, L. Zsolnai, G. Huffner and H. H. Brintzinger, J. Organomet. Chem., 232 (1982) 233.
3 W. Kaminsky, K. Kulper, H. H. Brintzinger and F. R. W. P. Wild, Angew. Chem., 97 (1985) 507.
4 R. A. Shanks and K. M. Drummond, Annu. Tech. Conf.-Soc. Plas. Eng., 56th (vol. 2) (1998) 2004.
5 Y. M. Kim, C. H. Kim, J. K. Park, J. W. Kim and T. I. Min, J. Appl. Polym. Sci., 60(13) (1996) 2469.
6 V. B. F. Mathot and M. F. J. Pijpers, J. Appl. Polym. Sci., 39(4) (1990) 979.
7 S. A. Karoglanian and I. R. Harrison, Polym. Eng. Sci., 36(5) (1996) 731.
8 E. Karbashewski, L. Kale, A. Rudin, W. J. Tchir, D. G. Cook and J. O. Pronovost, J. Appl. Polym. Sci., 44(3) (1992) 425.
9 G. Balbontin, I. Camurati, T. Dall'Occo, A. Finotti, R. Franzese and G. Vecellio, Angew. Makromol. Chem., 219 (1994) 139.
10 V. Mathot, T. Pijpers and W. Bunge, Polym. Mater. Sci. Eng., 67 (1992) 143.
11 D. R. Parikh, B. S. Childress and G. W. Knight, Annu. Tech. Conf.-Soc. Plast. Eng., 49th (1991) 1543.
12 F. Cser, J. L. Hopewell and R. A. Shanks, J. Therm. Anal. Cal., 54 (1998) 707.
13 M. Y. Keating, I. H. Lee and C. S. Wong, Thermochim. Acta, 284(1) (1996) 47.
14 M. Y. Keating and E. F. McCord, Thermochim. Acta, 243(2) (1994) 129.
15 P. Starck, Polymer International, 40(2) (1996) 111.
16 B. Wolf, S. Kenig, J. Klopstock and J. Miltz, J. Appl. Polym. Sci., 62(9) (1996) 1339.
17 F. H. Chiu, M. Y. Keating and S. Z. D. Cheng, Proceeding of AMTEC, (1995) 1503
18 Z. G. Wang, B. S. Hsiao, J. Lopez and J. P. Armistead, J. Polym. Research, in press (1999).